Article citation info:
Goolak S, Gorobchenko O, Holub H, Dudnyk Y. Increasing the efficiency of railway rolling stock operation with induction traction motors due to implementation of the operational system for diagnostic condition of rotor. Diagnostyka. 2024;25(4):2024404.
https://doi.org/10.29354/diag/193809.

DIAGNOSTYKA, 2024, Vol. 25, No. 4

e-ISSN 2449-5220
DOI: 10.29354/diag/193809

INCREASING THE EFFICIENCY OF RAILWAY ROLLING STOCK OPERATION WITH INDUCTION TRACTION MOTORS DUE TO IMPLEMENTATION OF THE OPERATIONAL SYSTEM FOR DIAGNOSTIC CONDITION OF ROTOR

Sergey GOOLAK [1,*], Oleksandr GOROBCHENKO [1], Halyna HOLUB [2], Yuriy DUDNYK [3]

[1] Department of Electromechanics and Rolling Stock of Railways, State University of Infrastructure and Technologies (04071), Ukraine
[2] Department of Automation and Computer-Integrated Transport Technologies, State University of Infrastructure and Technologies (04071), Ukraine
[3] Department of Management, Public Administration and Administration, State University of Infrastructure and Technologies (04071), Ukraine
[*] Corresponding author, e-mail: sgoolak@gmail.com

Abstract

Traction drives with vector control are widely used on mainline locomotives with induction motors. Traction motors can fail due to malfunctions that occur during the operation of locomotives. Real-time functional diagnostic systems are necessary to prevent the failure of traction motors. The implementation of such systems will allow to detect the occurrence of malfunctions in the traction motor at the initial stage and prevent the further development of the defect. In the work, a structural diagram of functional diagnostics for monitoring the condition of the rotor of an induction motor is proposed and an algorithm for its operation is developed.

Keywords: operational efficiency, rolling stock, operational diagnostics, induction motor, rotor winding

1. INTRODUCTION

The railway belongs to the objects of critical infrastructure. Rolling stock is an element of critical infrastructure. Increasing the efficiency of operation of critical infrastructure facilities is always an urgent task [1-3].

The use of a diagnostic system [4] built into the traction drive of rolling stock is one of the ways to increase the efficiency of its operation. Such systems were called operational diagnostic systems.

On railway rolling stock, the traction drive system suffers the most damage [5]. Traction motors are the most damaged elements of the traction drive system [6, 7].

The rotor of an induction motor (IM) is one of its most damaged elements, as evidenced by the analysis of the data given in [8-10]. Statistics of induction motor failures are given in [10] (Fig. 1).

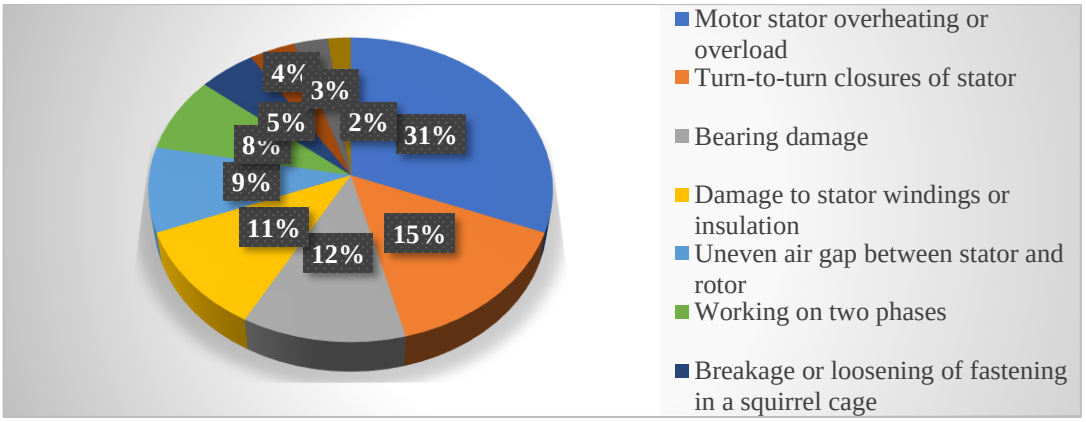

Fig. 1. Results of the analysis of the causes of emergency failures of induction motors with a squirrel-cage rotor

Received 2024-04-01; Accepted 26.09.2024; Available online 2024-10-22

From Fig. 1 it follows that a significant number of asynchronous motor failures are due to rotor failures (about 8%).

A large number of studies are devoted to the diagnosis of the condition of the rotor of an IM.

Diagnosing the condition of the rotor based on the spectral analysis of the stator currents of an IM is proposed in works [11-13]. Works [14-16] are devoted to diagnosing the condition of the rotor based on the analysis of magnetic flux harmonics. To solve the problem of monitoring the rotor state, methods of vibration diagnostics are proposed in works [17-19].

The listed methods will be effective when building a bench diagnostic system. When building a system of functional diagnostics, they will be ineffective. This is caused by the following factors:

- torque pulsations and imbalance of phase currents of an IM are a consequence of the asymmetry of its windings [20];
- the asymmetry of the stator phase voltages leads to the same consequences [21].

Autonomous voltage inverters are used to organize the system of phase voltages of the stator of an IM. The implementation of the pulse width modulation (PWM) algorithm is the basis of the operation of autonomous voltage inverters. Therefore, the spectra of the stator phase currents contain higher harmonics. The presence of higher harmonics in the spectra of the stator phase currents of an IM is due to the non-sinusoidal nature of the phase voltages of the stator as well.

That is, the use of the methods proposed in studies [11-13] and [14-16] in the construction of diagnostic systems will be effective when the phase voltages of the stator of an IM are symmetrical and sinusoidal. During the operation of railway rolling stock, there is a constant change in its modes of operation. Changing operating modes causes constant unstable modes in the traction drive of the rolling stock. In turn, unstable modes determine the presence of quasi-asymmetric modes of the system of phase voltages of the stator of an IM. That is why it is impossible to ensure symmetry and sinusoidal phase voltages of the stator of an IM [22].

In [23], a method of analysing stator currents is proposed, the use of which will allow developing a system for diagnosing the condition of the rotor of an IM during the operation of the rolling stock. The Park vector is used to diagnose the condition of an IM rotor in this research.

But the work [23] does not take into account the fact that the dynamic characteristics of the rolling stock work depend on its modes [24-26]. That is, a constant change in the traction motor load.

The article [27] is devoted to the research of the condition of the windings of an IM with a constant load change. But in it, the authors proposed only an algorithm without technical solutions.

The use of vibration methods for operational diagnosis of the condition of the rotor of an IM is also ineffective. The largest torque pulsations in the presence of asymmetry in the windings of an IM will be in the idling mode [20]. In the traction drive of railway rolling stock, the traction motors are always under load. In addition, for the application of vibration diagnostics methods, it is necessary to have a priori information about the vibration spectrum of an IM [28]. The listed factors make it difficult to use vibration methods to build an operational diagnostic system for monitoring the condition of the windings of an IM.

Control of the value of the angular speed of rotation of the shaft of an IM can be another approach in the development of a system for diagnosing the condition of the rotor [29-31]. This fact is possible because damage to the rotor causes an increase in power loss in it [32-34]. This will lead to increased slippage in the IM.

IMs with a short-circuited rotor are most widely used in railway rolling stock. Systems with scalar control [35-37], vector control [38-40] and direct torque control [41-43] can be used to control IMs. The organization of the traction drive system should also be taken into account when developing a system for operational diagnostics of the condition of the rotor of an IM.

The vector control system is the most effective for mainline rolling stock [38]. The vector control system includes a flux linkage observer unit. The induction motor slip is calculated in this unit. That is, when building a system for operational diagnosis of the condition of the rotor of an IM and the basis of slip control in the vector control system, it is necessary to make minor structural changes in the schematic diagram.

The relevance of the study is caused by the need to detect defects in the rotor windings at an early stage, taking into account the operating states and the need to turn off the traction motor when the rotor is damaged. This circumstance is important due to the fact that rotor malfunctions will lead to damage to other elements of the induction motor and, as a result, to an increase in the cost of repairs, and even to a complete replacement of the motor.

2. THE AIM AND OBJECTIVES OF RESEARCH

The aim of the research is to develop a system for functional diagnostics of the condition of the rotor of an IM in the traction drive of railway rolling stock.

The following tasks were solved to achieve the set aim:

- the existing methods of monitoring the condition of the rotor were analysed. It is proposed to use the amount of slip as a diagnostic parameter for monitoring the condition of the rotor;
- a structural diagram for diagnosing the condition of the rotor was developed;
- a structural diagram of the unit for diagnosing the condition of the rotor was developed;

- it is proposed to supplement the basic scheme of vector control of IMs with a unit for diagnosing the condition of the rotor;
- obtained dependences of rotor slip on the angular frequency of the motor shaft rotation for cases of an undamaged rotor and for different degrees of rotor damage;
- the operation algorithm of the rotor condition diagnostics unit was proposed on the basis of the obtained dependences of the rotor slip on the frequency of rotation of the shaft of an IM.

3. THE OBJECT OF RESEARCH AND ITS MAIN PARAMETERS

The traction drive of the DS-3 series electric locomotive (Ukraine) with a vector control system for IMs was chosen as the research object [38].

The simulation model of the traction drive system of the DS-3 series electric locomotive is given in the research [38]. It is implemented in the MATLab software environment. Therefore, it is inappropriate to present its diagram in this research.

DS-3 electric locomotives are equipped with IMs from the STA-1200 series. Table 1 presents their parameters [44].

There are many approaches to modeling three-phase induction motors. This is a model in two-phase stationary coordinates (αβ coordinates) [45-47], in two-phase moving coordinates directed along the rotor field (dq coordinates) [48-50], three-phase stationary coordinates [51-53] and others.

Table 1. Main parameters of the IM STA-1200 series

Parameter	Unit	Value
Power P	kW	1200
The effective value of the line voltage U_l	V	1870
The actual value of the stator phase current I_s	A	450
Nominal frequency of the supply voltage f_{nom}	Hz	55.8
Number of phases m	number	3
Number of pole pairs p	number	3
Nominal rotation frequency	rpm	1110
Torque, T	N·m	10700
Efficiency η	%	95.5
Power factor cosφ	r. u.	0.88
Active resistance of the stator winding r_s	Ω	0.0226
Active resistance of the rotor windings brought to the stator winding r'_r	Ω	0.0261
Dissipation inductance of the stator winding L_s	mH	0.65
Dissipation inductance of the rotor winding brought to the stator winding L'_r	mH	0.45
Total inductance of the magnetization circuit L_μ	mH	19.4336
Moment of inertia J	kg·m^2	39

Each of the models has its advantages and disadvantages. They can be effective for solving one problem and unsuitable for solving another problem. On models made in two-phase coordinates [45-47] and [48-50], it is difficult to organize the asymmetry of the windings of an IM. But these works do not provide an algorithm for implementing the asymmetry of the windings of an IM. In works [44, 54], based on the methodology proposed in work [55], an algorithm for implementing the asymmetry of the windings of an IM is given.

Therefore, for further research, a simulation model of an IM was chosen, which is given in the paper [44]. The diagram of the simulation model of an IM, which is implemented in the MATLab software environment, is given in the work [44].

Therefore, it is inappropriate to mention it in this work.

4. DEVELOPMENT OF THE ROTOR CONDITION DIAGNOSTIC UNIT AS PART OF THE VECTOR CONTROL SYSTEM OF AN IM

In the basic vector control system, the rotor slip is calculated in the "Rotor flux linkage observer" block based on the values of the stator phase currents and the value of the angular frequency of rotation of the motor shaft [56-58]. Therefore, additional input signals are unnecessary for the organization of the "Unit for diagnosing the condition of the rotor". To display information about the state of the rotor, the "Indication unit" should be used. Then the vector control scheme with the system of functional diagnosis of the condition of the rotor windings takes the form shown in Fig. 2.

The IM receives power from the inverter (Fig. 2). This leads to the appearance of higher harmonics in the spectra of the stator phase currents. Taking into account the fact that in traction drive systems, the sampling frequency in the organization of PWM is limited to 1 kHz [38], the amplitudes of the higher harmonics of the phase currents are quite significant. This causes the occurrence of torque pulsations, which lead to pulsations of the motor shaft rotation frequency and, as a result, to rotor slip pulsations [38]. The asymmetry of the rotor windings also causes torque pulsations [59-61]. In other words, both the power system based on the autonomous voltage inverter and damage to the rotor lead to the appearance of slip pulsations. This circumstance makes it difficult to diagnose the condition of the rotor windings by the values of the stator phase currents. Therefore, it is proposed to diagnose the condition of the rotor by the first harmonics of the stator phase currents. For this purpose, the "Unit for diagnosing the condition of the rotor" uses the "Fast Fourier transform unit" (Fig. 3).

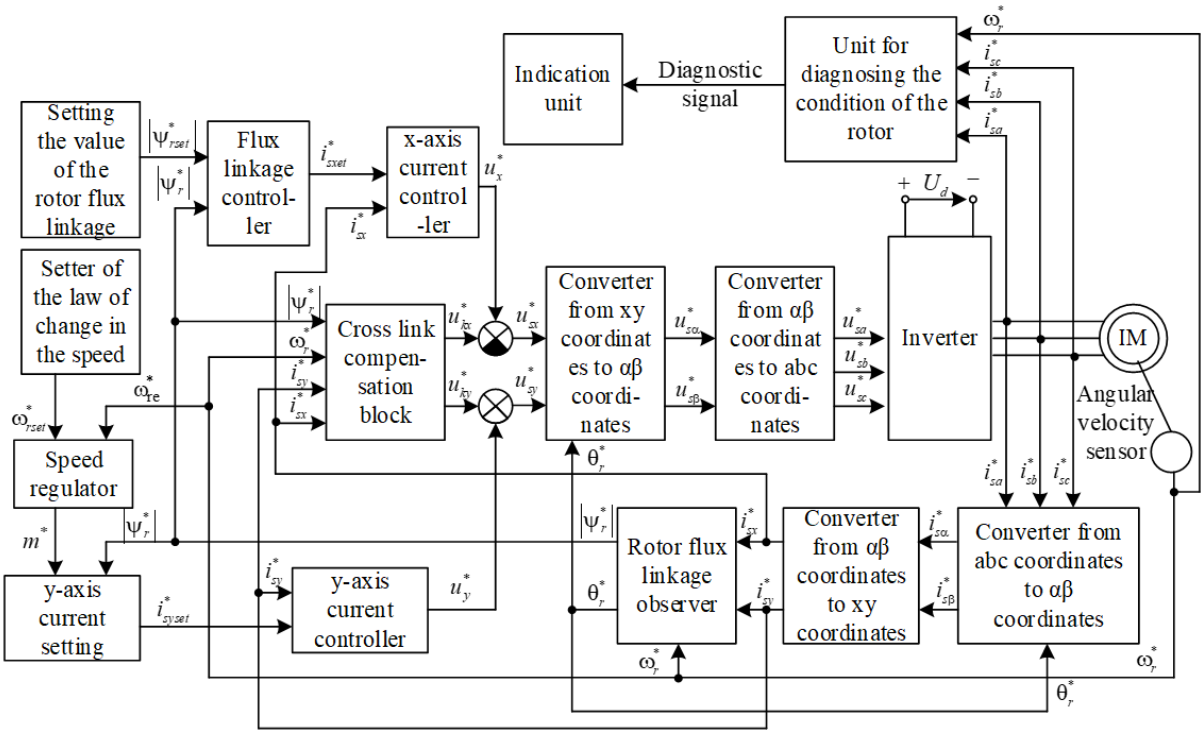

Fig. 2. Structural diagram of the vector control system with a unit for diagnosing the condition of the rotor of an IM

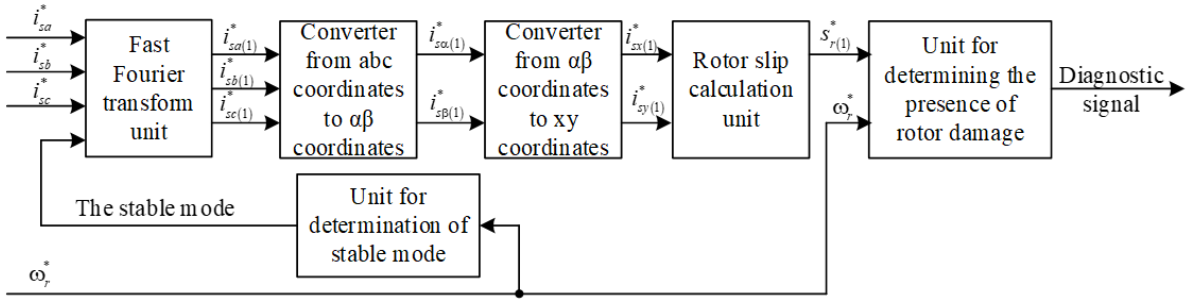

Fig. 3. Structural diagram of the unit for diagnosing the condition of the rotor

Operating modes of rolling stock constantly change during operation. In this regard, unstable modes are present in the traction drive system for a considerable time. This fact can lead to errors during diagnosis. To determine the stable mode of operation of the traction drive system, the "Unit for determination of stable mode" is used in the "Unit for diagnosing the condition of the rotor " (Fig. 3), the signal from which turns on the "Fast Fourier transform unit". The first harmonics of the stator phase currents from the "Fast Fourier transform unit" are sent to the "Converter from *abc* coordinates to αβ coordinates". The stator phase currents in αβ coordinates from the "Converter from *abc* coordinates to αβ coordinates" unit are sent to the "Converter from αβ coordinates to *xy* coordinates". The stator phase currents in *xy* coordinates are formed at the output "Converter from αβ coordinates to *xy* coordinates".

In the "Rotor slip calculation unit" the value of rotor slip is calculated according to the formula [59]

$$s = \frac{r_r \cdot k_r}{|\psi_{rx}|} \cdot i^*_{sy}, \tag{1}$$

where $|\psi_{rx}|$ - flux linkage module of the rotor along the *x* coordinate, *r. u.*;
k_r - rotor circuit coefficient, *r. u.*;
r_r - rotor chain resistance, *r. u.*;
i^*_{sy} - value of the stator current according to the y coordinate, *r. u.*

The flux linkage module of the rotor along the *x* coordinate is determined by the formula [59]

$$|\psi_{rx}| = \frac{l_\mu \cdot k_r}{\frac{T_r}{\Omega_b} \cdot p + 1} \cdot i^*_{sx}, \tag{2}$$

where l_μ - inductance of the magnetic circuit, *r. u.*;
T_r - time constant of the rotor circuit, *r. u.*;
Ω_b - basic value of the angular frequency of phase voltages of the stator, s^{-1};
i^*_{sx} - value of the stator current according to the *x* coordinate, *r. u.*;
p - Laplace operator.

The basic value of angular frequency of phase voltages of the stator is determined by the formula [38]

$$\Omega_b = 2 \cdot \pi \cdot f_{nom} = 360.6, s^{-1}, \quad (3)$$

where f_{nom}=55.8 - the nominal frequency of the phase voltages of the stator (Table 1), *Hz*.

Magnetic circuit inductance in relative units [38]

$$l_\mu = \frac{\Omega_b \cdot L_\mu}{Z_b} = 2.839, r.u., \quad (4)$$

where L_μ=19.4336 - the inductance of the magnetic circuit (table 1), *mH*;
Z_b - basic resistance value, *Ω* [38]:

$$Z_b = \frac{U_{fnom}}{I_{fnom}} = \frac{U_{lnom}}{\sqrt{3} \cdot I_{fnom}} = 2.4, \Omega, \quad (5)$$

where U_{lnom}=1870 - effective value of the line voltage (Table 1), *V*;
I_{fnom}=450 - effective value of the phase current (table 1), *A*.

The time constant of the rotor circuit is determined in accordance with the expression [38]

$$T_r = \frac{l_\mu + l_{r\sigma}}{r_r} = 276.32, r.u., \quad (6)$$

where $l_{r\sigma}$ - dissipation inductance of the rotor winding is in relative units [38]:

$$l_{r\sigma} = \frac{\Omega_b \cdot L_{r\sigma}}{Z_b} = 0.066, r.u., \quad (7)$$

where $L_{r\sigma}$=0.45 - dissipation inductance of the rotor winding, reduced to the stator winding (Table 1), *mH*.

Rotor circuit resistance in relative units [38]:

$$r_r = \frac{R'_r}{Z_b} = 0.010875, r.u., \quad (8)$$

where R'_r=0.0261 - resistance of the rotor circuit of the rotor winding, reduced to the stator winding (Table 1), Ω.

Rotor circuit coefficient [38]

$$k_r = \frac{l_\mu}{l_\mu + l_{r\sigma}} = 0.9773, r.u., \quad (9)$$

Since when determining the rotor slip for the basic scheme there were slip pulsations caused by the reasons discussed above, for this case the average value of the slip was determined:

$$s_{r\_av} = \frac{s_{rmax} + s_{rmin}}{2}, \quad (10)$$

where s_{rmax} - the maximum value of rotor slip, *relative units*;
s_{rmin} - the minimum rotor slip value, *relative units*.

The slip of the IM rotor is determined according to the equation

$$s_r = \frac{\omega_{rsynchr} - \omega_{rasynchr}}{\omega_{rsynchr}}, \quad (11)$$

where $\omega_{rsynchr}$ – synchronous angular frequency of rotation of the rotor, *rag/s*;
$\omega_{rasynchr}$ - asynchronous angular frequency of rotation of the rotor, *rag/s*.

Dependencies of the rotor slip of the IM and the slip calculated in the "Rotor slip calculation unit" (Fig. 3) on the electrical angular frequency of rotation of the rotor are obtained as a result of simulation.

For both cases, the simulation was performed for the following supply voltage frequencies:

1. At a frequency f=0.9·f_{nom};
2. At a frequency f=0.95·f_{nom};
3. At nominal frequency;
4. At a frequency f=1.05·f_{nom};
5. At a frequency f=1.1·f_{nom};

The results of modeling and calculations are listed in Table 2.

Table 2. Results of determination of rotor slip as a function of engine shaft rotation frequency with an intact rotor

Frequency of stator phase voltages *f*, *Hz*	Experiment			
	Electric angular frequency of rotation of the rotor ω_{r1}, *rag/s*	Slip s_1, r. u.	Electric angular frequency of rotation of the rotor ω_r, *rag/s*	Slip *s*, r. u.
50.22	313.755	0.005656	313.832	0.005412
53.01	331.192	0.005638	331.273	0.005394
55.8	348.630	0.00562	348.715	0.005376
58.59	366.068	0.005601	366.160	0.005357
61.38	383.507	0.005582	383.602	0.005338

The dependences of AD rotor slip (s1=f(ω1)) and slip calculated in the "Rotor Slip Calculation Block" (s=f(ω)) on the electrical angular frequency of the stator phase voltages (Fig. 4) are obtained according to the results of Table. 2.

As can be seen from Fig. 4, at the same electrical angular frequencies of the phase voltages of the stator, the slip of the IM has a greater value than that calculated in the "Rotor slip calculation unit". This is explained by the effect of higher harmonics of the stator phase currents on losses in the IM, and therefore on slip.

Since the dependences of the slip on the electric angular frequency of the stator phase voltages are linear, for the proposed scheme their analytical expression will have the form

$$s_r = 1 - \frac{s_{r(53.01)} - s_{r(55.8)}}{\omega_{r(55.8)} - \omega_{r(53.01)}} \cdot \omega_r = \\ = 1.032 \cdot 10^{-6} \cdot \omega_r, \quad (12)$$

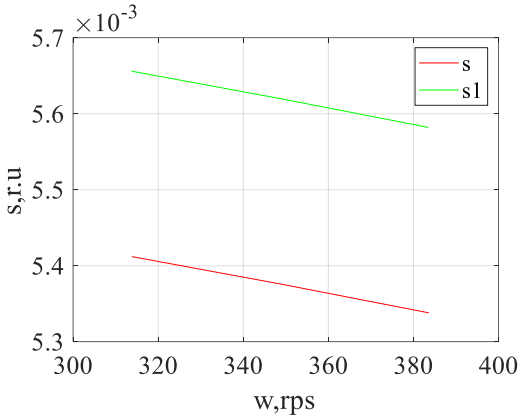

Fig. 4. Dependencies of the rotor slip of the IM (s1=f(ω1)) and the slip calculated in the "Rotor slip calculation unit" (s=f(ω)) on the electric angular frequency of rotation of the rotor

where $s_{r(53.01)}$=0.005394 - slip corresponding to the frequency of the stator phase voltages of 53.01 *Hz* (Table 2), *r. u*;
$s_{r(55.8)}$=0.005376 - slip corresponding to the nominal frequency of the stator phase voltages of 55.8 *Hz* (Table 2), *r. u.*;
$\omega_{r(55.8)}$=348.715 - electric angular frequency of phase voltages of the stator, which corresponds to the nominal frequency of 55.8 *Hz* (Table 2), *rps*;
$\omega_{r(53.01)}$=331.273 - electric angular frequency of phase voltages of the stator, which corresponds to the nominal frequency of 53.01 *Hz* (Table 2), *rps*.

In accordance with expression (11), the value of slip for an undamaged rotor is calculated in the "Unit for determining the presence of rotor damage", which is compared with the value calculated in the "rotor slip calculation unit". If the slip values calculated in the "Unit for determining the presence of rotor damage" and in the "Rotor slip calculation unit" match, the "Indication Unit" receives a signal of the absence of damage in the rotor, if they differ, the "Indication Unit" receives a signal of the presence of damage in the rotor.

5. DEVELOPMENT OF THE FUNCTIONING ALGORITHM OF THE UNIT FOR DIAGNOSTIC STATE OF THE ROTOR

The operation of the "Rotor condition diagnostic unit" is based on the algorithm for determining the presence of damage in the rotor of an IM. For its development, it is necessary to establish the dependence of slip on the electrical angular frequency of rotation at different degrees of damage to the rotor. It is also necessary to determine the accuracy with which the rotor slip should be calculated and the limits of deviation of the slip values calculated in the "Unit for determining the presence of rotor damage" and in the "Rotor slip calculation unit".

Four experiments were conducted to answer the question about the dependence of the rotor slip on the electrical angular frequency of rotation in the presence of damage in the rotor.

For the supply voltage frequency values used in the previous experiments, the results of the following experiments were recorded on the simulation model implemented for the case of the proposed scheme:
1. one rotor rod is damaged;
2. two rotor rods are damaged;
3. three rotor rods are damaged;
4. four rotor rods are damaged.

Since slip pulsations are present when the rotor is damaged, the average values of rotor slip were calculated using formula (10). The results are listed in Table 3.

According to the results of Table 3, graphs of the dependence of the rotor slip on the angular speed of the motor shaft rotation in the presence of damage to the rotor windings for different degrees of damage are plotted (Fig. 5).

As can be seen from Fig. 5, the dependences of the rotor slip on the electrical angular speed of rotation in the presence of rotor damage for different degrees of damage are also linear. Moreover, with an increase in the degree of damage, at the same frequency of phase voltages of the stator, the slip increases.

Slip values are calculated in the "Unit for determining the presence of rotor damage" and in the "Rotor slip calculation unit". The slip values obtained are compared. In the event that the value calculated in the "Rotor slip calculation unit" is greater than the value calculated in the "Unit for determining the presence of rotor damage", the Ds signal equal to 1 is sent to the "Indication Unit". This fact indicates the presence of damage in the rotor. Otherwise, a Ds signal equal to 0 is sent to the "Indication Unit". This fact indicates the absence of damage in the rotor.

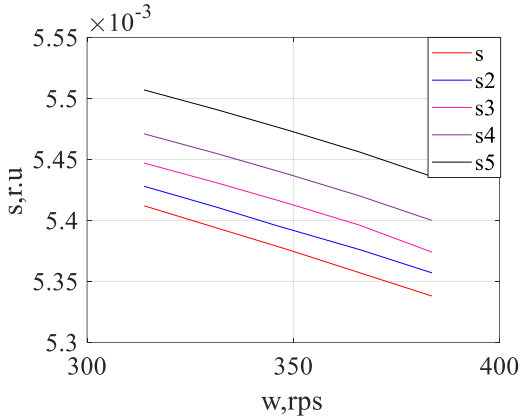

Fig. 5. Dependencies of slip on the electric angular frequency of rotation for different degrees of rotor damage: s2 – one rod is damaged; s3 – two rods are damaged; s4 – three rods are damaged; s5 –damaged four rods are damaged

Table 3. Results of determination of rotor slip as a function of engine shaft rotation frequency with a damaged rotor

Frequency of stator phase voltages *f, Hz*	Experiment							
	one rotor rod is damaged		two rotor rod is damaged		three rotor rod is damaged		four rotor rod is damaged	
	Electric angular frequency of rotation of the rotor ω_{r2}, *rps*	Slip s_2, *r. u.*	Electric angular frequency of rotation of the rotor ω_{r3}, *rps*	Slip s_3, *r. u.*	Electric angular frequency of rotation of the rotor ω_{r4}, *rps*	Slip s_4, *r. u.*	Electric angular frequency of rotation of the rotor ω_{r5}, *rps*	Slip s_5, *r. u.*
50.22	313.827	0.005428	313.821	0.005447	313.814	0.005471	313.802	0.005507
53.01	331.268	0.005411	331.261	0.005431	331.253	0.005455	331.241	0.005491
55.8	345.682	0.005396	348.702	0.005414	348.693	0.005438	348.681	0.005474
58.59	366.151	0.005376	366.144	0.005396	366.135	0.00542	366.121	0.005456
61.38	383.594	0.005357	383.587	0.005374	383.577	0.0054	383.564	0.005436

Taking into account the description of the operation of the structural diagram of the "Rotor slip calculation unit" and the above-mentioned nature of the change in the dependence of the rotor slip on the angular speed of rotation of the motor shaft in the presence of damage to the rotor windings, the operation algorithm of the "Rotor slip calculation unit" can be depicted as shown in Fig. 6.

The calculation of the difference limits of the values of rotor slip, calculated in the "Unit for determining the presence damage to the rotor windings" and "Rotor slip calculation unit" was carried out based on the following considerations. As can be seen from fig. 6, the dependences of the rotor slip on the angular speed of rotation of the motor shaft in the presence of damage and the absence of rotor windings are almost parallel. In addition, the smallest difference with the dependence of the rotor slip on the angular speed of rotation of the motor shaft in the absence of damage to the rotor windings has the specified characteristic for the case of damage to one rotor rod.

Then the difference of these characteristics for the same value of the supply voltage frequency will be equal

$$\Delta s_r = s_{r1(55.8)} - s_{r(55.8)} = 0.00002, r.u., \quad (13)$$

where $s_{r1(55.8)}$=0.005396 - slip at the nominal frequency of the stator phase voltages voltage for the case of damage to one rotor rod, *r. u.*;

$s_{r(55.8)}$=0.005376 - slip at the nominal frequency of the phase voltages of the stator in the absence of damage to the rotor, *r. u.*

The accuracy of the slip determination is chosen equal to half the difference between the values calculated in the "Unit for determining the presence of rotor damage" and in the "Rotor slip calculation unit", i. e. $ds_r=\Delta s_r/2$=0.00001. As can be seen from Table 6, the slip values are determined with accuracy up to the sixth digit. In other words, the sliding accuracy during the experiments was equal to $\delta_{s_r} = 10^{-6}$.

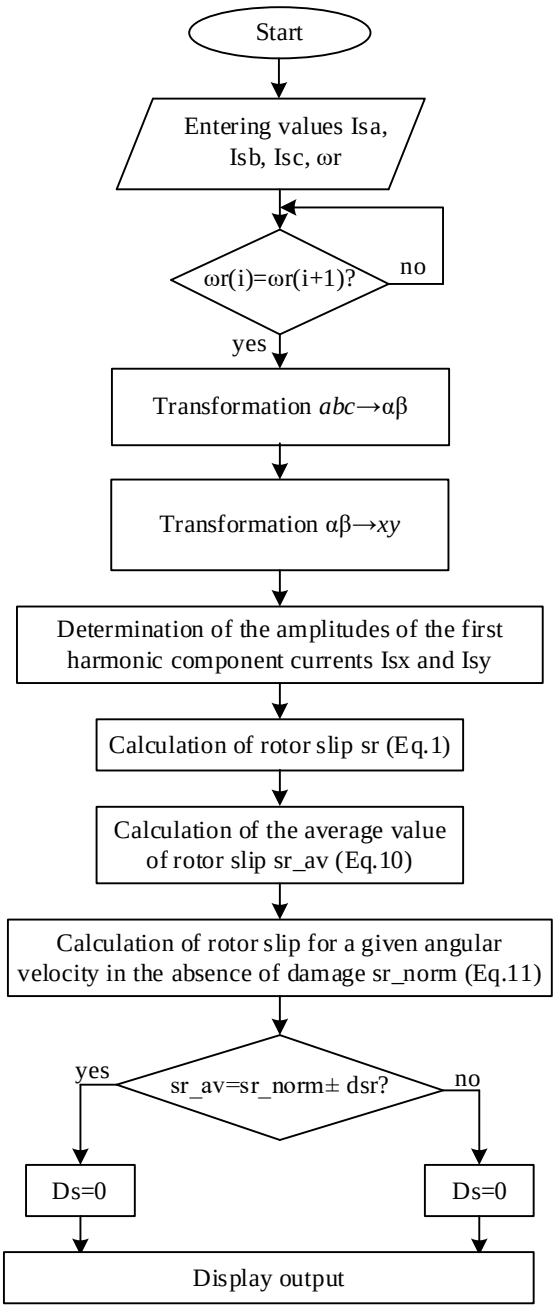

Fig. 6. Algorithm of "Rotor slip calculation unit" operation

It should be noted that the research was conducted for the case when a P-regulator, i. e. a proportional regulator, was used as a speed regulator in the vector control system. In some vector control systems, a PI controller is used as a speed controller. It is necessary to conduct additional studies to obtain the dependence of sliding on the electrical angular speed of rotation in the presence and absence of rotor damage in order to obtain correct results in this case. In the case when the nature of the specified dependencies differs from the linear one, the resulting dependencies should be approximated.

All other steps of the proposed algorithm remain the same.

6. CONCLUSION

In this study, a system of functional diagnosis of the condition of the rotor windings of an IM in the traction drive system of the electric rolling stock of railways was developed.

As a result of the analysis of scientific studies devoted to the diagnosis of induction motors, it was established that the use of the rotor slip value can be effective as a diagnostic feature in diagnosing the condition of the rotor windings. This made it possible to add to the structural diagram of the vector control system a block for diagnosing the condition of the IM rotor, the operation of which is based on the analysis of the rotor slip value.

As a result of the simulation, the dependences of the IM rotor slip and the slip calculated in the "Rotor slip calculation unit" on the electrical angular frequency of rotation of the rotor were obtained. From the analysis of the obtained dependencies, it follows that the error of the slip calculation in the "Rotor slip calculation unit" does not exceed 4.5%, which will allow obtaining the slip value with high accuracy and determining the presence of damage in the rotor windings with high reliability.

Based on the obtained dependence of the slip calculated in the "Rotor slip calculation unit" on the electrical angular frequency of rotation of the rotor, the accuracy with which it is necessary to calculate the slip is determined. Its value was 10^{-6}.

As a result of the simulation, the dependence of the slip calculated in the "Rotor slip calculation unit" on the electrical angular frequency of rotation for different degrees of rotor damage was obtained. The analysis of the obtained dependences showed that with the same frequency of the stator supply voltages, the value of the rotor slip increases as the degree of damage to the rotor windings increases. In addition, the smallest deviation of the slip value when the rotor windings are damaged from the slip value when the windings are intact will be when one rotor rod is damaged. The value of the deviation for this case is equal to Δs_{r1}=0.00002, which is much greater than the accuracy of determining the rotor slip (δ_s=10^{-6}). This fact makes it possible to state with high probability the presence of damage in the windings of the IM rotor.

The continuation of the research can be works devoted to the development of a comprehensive system for diagnosing the condition of traction drive elements of railway rolling stock.

Source of funding: *The article was written within the framework of the Project 2022.01/0224 "Development of scientific principles for comprehensive improvement of safety, efficiency of operation and management of critical railway transport facilities in the conditions of post-war development of Ukraine" under the competition "Science for the reconstruction of Ukraine in the war and post-war periods" with the financial support of the National Research Foundation of Ukraine.*

Author contributions: *research concept and design, S.G., H.H., Y.D.; Collection and/or assembly of data, O.G., H.H., Y.D.; Data analysis and interpretation, S.G., O.G., H.H., Y.D.; Writing the article, S.G.; Critical revision of the article, O.G.; Final approval of the article, S.G., O.G., H.H., Y.D.*

Declaration of competing interest: *The authors declare that they have no known competing financial interests or personal relationships that could have appeared to influence the work reported in this paper.*

REFERENCES

1. Bondarenko I, Severino A, Olayode IO, Campisi T, Neduzha L. Dynamic sustainable processes simulation to study transport object efficiency. Infrastructures 2022; 7(9): 124. https://doi.org/10.3390/infrastructures7090124.
2. Kulbovskyi I, Holub H, Sapronova S, Bambura O. Modeling of metrological support of qualimetric measurements on transport objects. Transport Means - Proceedings of the International Conference 2021; 886–889.
3. Holub H, Kulbovskyi I, Kharut V, Tkachuk M, Tymoshchuk O. Methods of intelligent data processing of the system of control and diagnostics of electric power transport objects. Transport Means - Proceedings of the International Conference 2021; 797–801.
4. Komorski P, Kominowski J, Motyl M. A proposal for a mobile system of vehicle and rail track diagnostics. Transport Problems 2022; 17(2): 46–56. https://doi.org/10.20858/tp.2022.17.2.04.
5. Yakubov MS, Turdibekov KKh, Norzhigitov SA, Sagatova MA. Improving maintenance system for controlled asynchronous electric drives of electric locomotives based on their diagnosis. E3S Web of Conferences 2023; 401: 05019. https://doi.org/10.1051/e3sconf/202340105019.
6. Pennacchi P, Chatterton S, Vania A, Xu L. Diagnostics of bearings in rolling stocks: results of long lasting tests for a regional train locomotive. Proceedings of the 10th International Conference on Rotor Dynamics – IFToMM 2019; 61; 321–35. https://doi.org/10.1007/978-3-319-99268-6_23.
7. Li Y, Li H, Fei J, Lu C, Ma J. Composite fault diagnosis method of EMU traction motor speed sensor considering harmonic interference. International

Journal of Heavy Vehicle Systems 2022; 29(4): 424. https://doi.org/10.1504/IJHVS.2022.127812.
8. Liang X, Ali MZ, Zhang H. Induction motors fault diagnosis using finite element method: A Review. IEEE Transactions on Industry Applications 2020; 56(2): 1205–17. https://doi.org/10.1109/TIA.2019.2958908.
9. Husach S, Yatsiuk R, Mamchur D. Induction motors operation condition evaluation and damage degree estimation methods. 2020 IEEE Problems of Automated Electrodrive. Theory and Practice (PAEP) 2020; 1–4. https://doi.org/10.1109/PAEP49887.2020.9240883.
10. Gubarevych O, Goolak S, Golubieva S. Systematization and selection of diagnosing methods for the stator windings insulation of induction motors. Revue Roumaine des sciences techniques—série électrotechnique et énergétique 2022; 67(4): 445-450.
11. Amanuel T, Ghirmay A, Ghebremeskel H, Ghebrehiwet R, Bahlibi W. Comparative analysis of signal processing techniques for fault detection in three phase induction motor. Journal of Electronics and Informatics 2021; 3(1): 61–76. https://doi.org/10.36548/jei.2021.1.006.
12. Saad K, Ali TB, Abdellah K. Detection and diagnosis of rotor and stator faults in open end winding induction motor. 2019 1st International Conference on Sustainable Renewable Energy Systems and Applications (ICSRESA) 2019; 1–5. https://doi.org/10.1109/ICSRESA49121.2019.9182560.
13. Trujillo Guajardo LA, Platas Garza MA, Rodríguez Maldonado J, González Vázquez MA, Rodríguez Alfaro LH, Salinas Salinas F. Prony method estimation for motor current signal analysis diagnostics in rotor cage induction motors. Energies 2022; 15(10): 3513. https://doi.org/10.3390/en15103513.
14. Sapena-Bano A, Martinez-Roman J, Puche-Panadero R, Pineda-Sanchez M, Perez-Cruz J, Riera-Guasp M. Induction machine model with space harmonics for the diagnosis of rotor eccentricity, based on the convolution theorem. International Journal of Electrical Power & Energy Systems 2020; 117: 105625. https://doi.org/10.1016/j.ijepes.2019.105625.
15. Antonino-Daviu J, Zamudio-Ramirez I, Osornio-Rios RA, Fuster-Roig V, De JesusRomero-Troncoso R, Dunai LD. Stray flux analysis for the detection of rotor failures in wound rotor induction motors. IECON 2019 - 45th Annual Conference of the IEEE Industrial Electronics Society 2019; 3704–9. https://doi.org/10.1109/IECON.2019.8927619.
16. Skowron M, Orłowska-Kowalska T. Efficiency of cascaded neural networks in detecting initial damage to induction motor electric windings. Electronics 2020; 9(8): 1314. https://doi.org/10.3390/electronics9081314.
17. Garcia-Calva T, Morinigo-Sotelo D, Fernandez-Cavero V, Romero-Troncoso R. Early Detection of Faults in Induction Motors – A review. Energies 2022; 15(21): 7855. https://doi.org/10.3390/en15217855.
18. Jorkesh S, Poshtan J. Fault diagnosis of an induction motor using data fusion based on neural networks. IET Science, Measurement & Technology 2021; 15(8): 681–9. https://doi.org/10.1049/smt2.12068.
19. Kabul A, Unsal A. A diagnosis method of multiple faults of induction motors based on vibration signal analysis. 2021 IEEE 13th International Symposium on Diagnostics for Electrical Machines, Power Electronics and Drives (SDEMPED) 2021; 415–21. https://doi.org/10.1109/SDEMPED51010.2021.9605511.
20. Gubarevych O, Goolak S, Daki E. Investigation of turn-to-turn closures of stator windings to improve the diagnostics system for induction motors. Problems of the Regional Energetics 2021; 2(50). https://doi.org/10.52254/1857-0070.2021.2-50.02.
21. Goolak S, Gubarevych, O, Gorobchenko, O, Nevedrov, O, Kamchatna-Stepanov K. Investigation of the influence of the quality of the power supply system on the characteristics of an asynchronous motor with a squirrel-cage rotor. Przegląd Elektrotechniczny 2022;1(6):144–50. https://doi.org/10.15199/48.2022.06.26.
22. Goolak S, Liubarskyi B, Lukoševičius V, Keršys R, Keršys A. Operational diagnostics system for asymmetric emergency modes in traction drives with direct torque control. Applied Sciences 2023; 13(9): 5457. https://doi.org/10.3390/app13095457.
23. Gubarevych O, Gerlici J, Kravchenko O, Melkonova I, Melnyk O. Use of Park's vector method for monitoring the rotor condition of an induction motor as a part of the built-in diagnostic system of electric drives of transport. Energies 2023; 16(13): 5109. https://doi.org/10.3390/en16135109.
24. Lovskaya A. Assessment of dynamic efforts to bodies of wagons at transportation with railway ferries. Eastern-European Journal of Enterprise Technologies 2014; 3(4(69)): 36. https://doi.org/10.15587/1729-4061.2014.24997.
25. Panchenko S, Gerlici J, Vatulia G, Lovska A, Pavliuchenkov M, Kravchenko K. The analysis of the loading and the strength of the flat rack removable module with viscoelastic bonds in the fittings. Applied Sciences 2022;13(1):79. https://doi.org/10.3390/app13010079.
26. Panchenko S, Vatulia G, Lovska A, Ravlyuk V, Elyazov I, Huseynov I. Influence of structural solutions of an improved brake cylinder of a freight car of railway transport on its load in operation. EUREKA: Physics and Engineering 2022(6): 45–55. https://doi.org/10.21303/2461-4262.2022.002638.
27. Gubarevych O, Goolak S, Daki O, Yakusevych Y. Determining an additional diagnostic parameter for improving the accuracy of assessment of the condition of stator windings in an induction motor. Eastern-European Journal of Enterprise Technologies 2021; 5(5(113)): 21–9. https://doi.org/10.15587/1729-4061.2021.239509.
28. Gubarevych O, Gerlici J, Gorobchenko O, Kravchenko K, Zaika D. Analysis of the features of application of vibration diagnostic methods of induction motors of transportation infrastructure using mathematical modeling. Diagnostyka 2023; 24(1): 1–10. https://doi.org/10.29354/diag/161308.
29. Pradhan PK, Roy SK, Mohanty AR. Detection of broken impeller in submersible pump by estimation of rotational frequency from motor current signal. Journal of Vibration Engineering & Technologies 2020; 8(4): 613–20. https://doi.org/10.1007/s42417-019-00165-6.
30. Braut S, Žigulić R, Skoblar A, Štimac Rončević G. Partial rub detection based on instantaneous angular speed measurement and variational mode decomposition. Journal of Vibration Engineering & Technologies 2020; 8(2): 351–64. https://doi.org/10.1007/s42417-019-00177-2.

31. Braut S, Žigulić R, Skoblar A, Štimac Rončević G. Fault detection based on instantaneous angular speed measurement and variational mode decomposition. MATEC Web of Conferences 2018; 211: 18006. https://doi.org/10.1051/matecconf/201821118006.
32. Do YN, Le TX, Nguyen NB, Ngo TT. Impact of asymmetrical phenomena on asynchronousthree-phase motors in operation mode. Journal of Mining and Earth Sciences 2020;61(3):68–74. https://doi.org/10.46326/JMES.2020.61(3).08.
33. Salah AA, Dorrell DG. Operating induction machine in DFIG mode including rotor asymmetry. 2019 southern african universities power engineering conference/robotics and mechatronics/pattern recognition association of south africa (SAUPEC/RobMech/PRASA) 2019; 469–74. https://doi.org/10.1109/RoboMech.2019.8704826.
34. El-Kharashi E, Massoud JG, Al-Ahmar MA. The impact of the unbalance in both the voltage and the frequency on the performance of single and cascaded induction motors. Energy 2019; 181: 561–75. https://doi.org/10.1016/j.energy.2019.05.169.
35. Fathy Abouzeid A, Guerrero JM, Endemaño A, Muniategui I, Ortega D, Larrazabal I, et al. Control strategies for induction motors in railway traction applications. Energies 2020; 13(3): 700. https://doi.org/10.3390/en13030700.
36. Ronanki D. Overview of Rolling Stock. Transportation Electrification 2022; 249–81. https://doi.org/10.1002/9781119812357.ch11.
37. Konowrocki R, Szolc T. An analysis of electromechanical interactions in the railway vehicle traction drive systems driven by ac motors. Research Methods and Solutions to Current Transport Problems 2020; 1032; 225–35. https://doi.org/10.1007/978-3-030-27687-4_23.
38. Goolak S, Liubarskyi B, Riabov I, Lukoševičius V, Keršys A, Kilikevičius S. Analysis of the efficiency of traction drive control systems of electric locomotives with asynchronous traction motors. Energies 2023;16(9):3689. https://doi.org/10.3390/en16093689.
39. Sakurazawa Y, Yamazaki O, Yuki K, Nakazawa Y, Natori K, Kondo K. Design of the speed sensorless field oriented control system for induction motors considering sudden change of the rotor speed. 2020 22nd European Conference on Power Electronics and Applications (EPE'20 ECCE Europe) 2020; 1-9. https://doi.org/10.23919/EPE20ECCEEurope43536.2020.9215959.
40. Nagataki M, Kondo K, Yamazaki O, Yuki K, Nakazawa Y. Online auto-tuning method in field-orientation-controlled induction motor driving inertial load. IEEE Open Journal of Industry Applications 2022;3:125–40. https://doi.org/10.1109/OJIA.2022.3189343.
41. Aktas M, Awaili K, Ehsani M, Arisoy A. Direct torque control versus indirect field-oriented control of induction motors for electric vehicle applications. Engineering Science and Technology, an International Journal 2020; 23(5): 1134–43. https://doi.org/10.1016/j.jestch.2020.04.002.
42. Maghfiroh H, Hermanu C. Optimal energy control of railway traction motor: Comparative study. 2019; 030020. https://doi.org/10.1063/1.5098195.
43. Ferestade I, Ahmadian M, Molatefi H, Moaveni B, Bokaeian V. Integrated sliding mode and direct torque controls for improving transient traction in high-speed trains. Journal of Vibration and Control 2021; 27(5–6): 629–50. https://doi.org/10.1177/1077546320932027.
44. Goolak S. Improvement of the model of an asynchronous traction motor of an electric locomotive by taking into account power losses. PRZEGLĄD ELEKTROTECHNICZNY 2022; 1(5): 3–12. https://doi.org/10.15199/48.2022.05.01.
45. Chung MV, Anh DT, Vu P. A finite set-model predictive control based on FPGA flatform for eleven-level cascaded H-Bridge inverter fed induction motor drive. International Journal of Power Electronics and Drive Systems (IJPEDS) 2021; 12(2): 845. https://doi.org/10.11591/ijpeds.v12.i2.pp845-857.
46. Aib A, Khodja DE, Chakroune S, Benyettou L. FPGA hardware in the loop validation of asynchronous machine with full direct torque control implementation. Advances in Modelling and Analysis B 2021; 64(1–4): 9–16. https://doi.org/10.18280/ama_b.641-402.
47. Lu J, Yang Z, Sun X, Bao C, Chen X. Direct levitation force control for a bearingless induction motor based on model prediction. IEEE Access 2019; 7: 65368–78. https://doi.org/10.1109/ACCESS.2019.2917331.
48. Purwanto E, Wahjono E, Ferdiansyah I, Yanaratri DS, Pradigta Setiya Raharja L, Eviningsih RP, et al. Implementation of genetic algorithm for induction motor speed control based on vector control method. 2019 International Seminar on Research of Information Technology and Intelligent Systems (ISRITI) 2019; 244–7. https://doi.org/10.1109/ISRITI48646.2019.9034674.
49. Németh Z, Kuczmann M. State space modeling theory of induction machines. Pollack Periodica 2020; 15(1): 124–35. https://doi.org/10.1556/606.2020.15.1.12.
50. Atiyah A, Sulc B. Role of asynchronous motor modelling in driven railway wheelset dynamical simulation model. 2020 21th International Carpathian Control Conference (ICCC) 2020; 1–6. https://doi.org/10.1109/ICCC49264.2020.9257241.
51. Li W, Xu Z, Zhang Y. Induction motor control system based on FOC algorithm. 2019 IEEE 8th Joint International Information Technology and Artificial Intelligence Conference (ITAIC) 2019; 1544–8. https://doi.org/10.1109/ITAIC.2019.8785597.
52. He F, Wang J, Yu W, Zhong G. Fault diagnosis of the three-phase asynchronous motor bond graph model based on bond graph and temporal causal graph. Journal of Physics: Conference Series 2023; 2428(1): 012017. https://doi.org/10.1088/1742-6596/2428/1/012017.
53. Liu Q, Zhang Z, Zhao D, Wang L, Meng F, Liu C. Research on speed tracking of asynchronous motor based on fuzzy control and vector control. 2020 39th Chinese Control Conference (CCC) 2020; 2144–9. https://doi.org/10.23919/CCC50068.2020.9188846.
54. Goolak S, Liubarskyi B, Sapronova S, Tkachenko V, Riabov Ie. Refined model of asynchronous traction electric motor of electric locomotive. Transport Means - Proceedings of the International Conference 2021: 455–460.
55. Goolak S, Gerlici J, Tkachenko V, Sapronova S, Lack T, Kravchenko K. Determination of Parameters of asynchronous electric machines with asymmetrical windings of electric locomotives. Communications - Scientific letters of the University of Zilina 2019; 21(2): 24–31. https://doi.org/10.26552/com.C.2019.2.24-31.
56. Ton TD, Hsieh MF. A Deadbeat current and flux vector control for IPMSM Drive with high dynamic

performance. Applied Sciences 2022; 12(8): 3789. https://doi.org/10.3390/app12083789.
57. Nair R, Gopalaratnam N. Stator Flux Based Model reference adaptive observers for sensorless vector control and direct voltage control of doubly-fed induction generator. IEEE Transactions on Industry Applications 2020: 1–1. https://doi.org/10.1109/TIA.2020.2988426.
58. Tang Q, Chen D, He X. Integration of improved flux linkage observer and i–f starting method for wide-speed-range sensorless SPMSM Drives. IEEE Transactions on Power Electronics 2020; 35(8): 8374–83. https://doi.org/10.1109/TPEL.2019.2963208.
59. Do NY, Ngo XC. Effects of voltage unbalance on matrix converter induction motor drive. Advances in Engineering Research and Application 2023; 602; 468–76. https://doi.org/10.1007/978-3-031-22200-9_53.
60. Yao K, Xiao H. Analysis of frequency control system in single-phase asynchronous motor. 2020 IEEE 1st China International Youth Conference on Electrical Engineering (CIYCEE) 2020; 1–7. https://doi.org/10.1109/CIYCEE49808.2020.9332777.
61. Suriano-Sánchez SI, Ponce-Silva M, Olivares-Peregrino VH, De León-Aldaco SE. A Review of torque ripple reduction design methods for radial flux PM motors. Eng 2022;3(4):646–61. https://doi.org/10.3390/eng3040044.
62. Rychlik A, Borecki M, Korwin-Pawlowski ML. Non-invasive method of car wheel rim examination. Proc. SPIE 10808, Photonics Applications in Astronomy, Communications, Industry, and High-Energy Physics Experiments 2018:08085S. https://doi.org/10.1117/12.2500627.

Sergey GOOLAK
PhD, Associate Professor
Department of Electromechanics and Rolling Stock of Railways of State University of Infrastructure and Technologies, Kyiv, Ukraine. Scientific interests – technical diagnostics of drives of transport systems.
E-mail: sgoolak@gmail.com

Oleksandr GOROBCHENKO
Doctor of Technical Sciences, Professor
Department of Electromechanics and Rolling Stock of Railways of State University of Infrastructure and Technologies, Kyiv, Ukraine. Scientific interests – human factor, rolling stock control and diagnostic systems.
E-mail: gorobchenko.a.n@gmail.com

Halyna HOLUB
PhD, Associate Professor
Department of Automation and Computer-Integrated Transport Technologies of State University of Infrastructure and Technologies, Kyiv, Ukraine. Scientific interests – control and diagnostics of rolling stock and power supply monitoring systems.
E-mail: holub.hm@gmail.com

Yuriy DUDNYK
PhD, Associate Professor
Department of Management, Public Administration and Administration of State University of Infrastructure and Technologies, Kyiv, Ukraine. Scientific interests – transportation technologies.
E-mail: yu.dudnyk@gmail.com